Molecular Biology of the Cell
Vol. 16, 3692–3704, August 2005

Phosphatidylinositol-4-Kinase Type II α Is a Component of Adaptor Protein-3-derived Vesicles[D]

Gloria Salazar,*† Branch Craige,*†‡ Bruce H. Wainer,§ Jun Guo,‖ Pietro De Camilli,‖ and Victor Faundez*¶

Departments of *Cell Biology and §Pathology and Laboratory Medicine, ‡Graduate Division of Biological and Biomedical Sciences, and ¶Center for Neurodegenerative Disease, Emory University, Atlanta, GA 30322; and ‖Howard Hughes Medical Institute and Department of Cell Biology, Yale University School of Medicine, New Haven, CT 06510

Submitted January 10, 2005; Revised May 11, 2005; Accepted May 31, 2005
Monitoring Editor: Keith Mostov

A membrane fraction enriched in vesicles containing the adaptor protein (AP) -3 cargo zinc transporter 3 was generated from PC12 cells and was used to identify new components of these organelles by mass spectrometry. Proteins prominently represented in the fraction included AP-3 subunits, synaptic vesicle proteins, and lysosomal proteins known to be sorted in an AP-3-dependent way or to interact genetically with AP-3. A protein enriched in this fraction was phosphatidylinositol-4-kinase type IIα (PI4KIIα). Biochemical, pharmacological, and morphological analyses supported the presence of PI4KIIα in AP-3-positive organelles. Furthermore, the subcellular localization of PI4KIIα was altered in cells from AP-3-deficient *mocha* mutant mice. The PI4KIIα normally present both in perinuclear and peripheral organelles was substantially decreased in the peripheral membranes of AP-3-deficient *mocha* fibroblasts. In addition, as is the case for other proteins sorted in an AP-3-dependent way, PI4KIIα content was strongly reduced in nerve terminals of *mocha* hippocampal mossy fibers. The functional relationship between AP-3 and PI4KIIα was further explored by PI4KIIα knockdown experiments. Reduction of the cellular content of PI4KIIα strongly decreased the punctate distribution of AP-3 observed in PC12 cells. These results indicate that PI4KIIα is present on AP-3 organelles where it regulates AP-3 function.

INTRODUCTION

Membrane-enclosed organelles possess distinctive protein compositions that are dynamically maintained by inbound and outbound vesicle carriers. These vesicles selectively concentrate appropriate membrane proteins while leaving behind resident proteins found in the donor organelle, a process called sorting (Bonifacino and Glick, 2004). Central to membrane protein sorting and vesiculation are a family of cytosolic coat complexes that mediate vesicle budding and function as cargo-specific adaptors. These include monomeric proteins and the heterotetrameric adaptor proteins (AP)-1, -2, -3, and -4 (Bonifacino and Glick, 2004; Robinson, 2004). These coats participate in the generation of vesicles that carry a unique array of membrane protein "cargoes." The characterization of these carriers has played a major role in the functional dissection of coat-dependent sorting and vesiculation mechanisms. For example, vesicles "in a basket" isolated from brain led to the biochemical identification of the first sorting machinery, clathrin and the AP-1 and AP-2 adaptors (Kanaseki and Kadota, 1969; Pearse, 1975; Pfeffer and Kelly, 1981; Pearse and Crowther, 1987). Subsequent studies of cargo molecules in brain clathrin-coated vesicles were crucial in revealing mechanisms of synaptic vesicle recycling (Pfeffer and Kelly, 1985; Maycox *et al*., 1992; Blondeau *et al*., 2004). The advent of complete genome sequencing and the concomitant development of informatics tools has led to the rapid identification of proteins by mass spectrometry (Taylor *et al*., 2003). Application of these methodologies to clathrin-coated vesicles has allowed the identification of new components involved in the clathrin-coated vesicle sorting machinery (Blondeau *et al*., 2004; Ritter *et al*., 2004). Collectively, these data show how purifying and analyzing enriched vesicle preparations can further our understanding of membrane traffic processes.

Biochemical purification of coated vesicles is facilitated when the desired fraction is abundant, but this approach has been more challenging for less abundant coat proteins such as AP-3. Fortunately, aspects of AP-3 function have been revealed by the AP-3 mouse mutants *mocha* (Kantheti *et al*., 1998; Kantheti *et al*., 2003) and *pearl* (Feng *et al*., 1999). Both *mocha* and *pearl* fail to assemble functional AP-3 complexes, and this defect is associated with impaired biogenesis of lysosomes and specialized secretory organelles, such as melanosomes, platelet-dense granules, lymphocyte cytotoxic granules, neutrophil granules (Dell'Angelica *et al*., 2000; Benson *et al*., 2003; Clark *et al*., 2003), and synaptic vesicle subpopulations (Kantheti *et al*., 1998, 2003; Nakatsu *et al*., 2004; Salazar *et al*., 2004a,b; Seong *et al*., 2005). In humans, genetic deficiencies in AP-3 function trigger the Hermansky–Pudlak type II syndrome; a disease that, like AP-3-deficiency in mice, is characterized by defective assembly of

This article was published online ahead of print in *MBC in Press* (http://www.molbiolcell.org/cgi/doi/10.1091/mbc.E05–01–0020) on June 8, 2005.

[D] The online version of this article contains supplemental material at *MBC Online* (http://www.molbiolcell.org).

† These authors contributed equally to this work.

Address correspondence to: Victor Faundez (faundez@cellbio.emory.edu).

lysosome/lysosome-related organelles, pigment dilution, and bleeding disorders (Dell'Angelica *et al*., 1999; Clark *et al*., 2003). However, despite knowledge of the organelles affected by the lack of functional APs, the molecular basis of the AP-3-deficient phenotypes is limited because only a subset of cargo proteins that are sorted by this complex has been identified (Dell'Angelica *et al*., 1999; Benson *et al*., 2003; Clark *et al*., 2003).

The AP-1 and AP-2 sorting machineries are far better understood because AP-1- and AP-2-coated vesicles can be isolated in large quantities. Numerous AP-1- and AP-2-binding proteins, their interactions with other components present in coated vesicles, and their functions have been precisely defined (Bonifacino and Traub, 2003; Robinson, 2004). The AP-3 sorting machinery has been characterized only to a limited extent due to the lack of preparations enriched in AP-3-coated vesicles or AP-3-derived vesicles. As a foundation to a systematic investigation of the biogenesis and function of AP-3 vesicles, we have now generated a subcellular fraction enriched in AP-3-derived vesicles and have carried out a proteomic analysis on this fraction. The concentration of phosphatidylinositol-4-kinase type IIα (PI4KIIα) in this fraction revealed by such analysis prompted us to characterize a potential link between this enzyme and AP-3. We report here morphological, genetic, biochemical, and pharmacological evidence indicating that PI4KIIα and AP-3 are functionally interconnected.

MATERIALS AND METHODS

Antibodies

The following antibodies were used: anti-synaptophysin (SY38; Chemicon International, Temecula, CA), anti-tubulin DM1A (Sigma, St. Lois, MO), anti-γ and -α adaptins, GM130, early endosome antigen (EEA) 1, and TGN38 (BD Biosciences, Franklin Lakes, NJ); anti-transferrin receptor (H68.4; Zymed Laboratories, South San Francisco, CA), anti-cathepsin D (Upstate Biotechnology, Charlottesville, VA), anti-KDEL receptor (StressGen Biotechnologies, San Diego, CA), anti-hemagglutinin (HA) (12CA5; a gift from Dr. Y. Altschuler, Tel Aviv University, Tel Aviv, Israel). Anti-SV2 (10H4), anti-mouse lysosomal-associated membrane protein (Lamp) I (ID4B), and anti-δ (SA4) were from the Developmental Studies Hybridoma Bank (University of Iowa, Iowa City, IA). Anti-116-kDa subunit of the vacuolar ATPase and VAMPII (69.1) were purchased from Synaptic Systems (Göttingen, Germany). AP-3 polyclonal antibodies, Arf1, and affinity-purified zinc transporter 3 (ZnT3) antibodies and sera have been already described (Salem *et al*., 1998; Faundez and Kelly, 2000; Salazar *et al*., 2004b). Monospecific affinity-purified polyclonal antibodies against phosphatidylinositol-4-kinase type IIα were reported by Guo *et al*. (2003).

Cell Culture

PC12 ZnT3-HA clone 4 cells were cultured following established procedures (Salazar *et al*., 2004b). Methyl-β-cyclodextrin (MβCD) treatment was performed as detailed below and in Salazar *et al*. (2004a,b). Importantly, MβCD treatment was performed in conditions that do not affect cell viability as determined by flow cytometry using the potentiometric mitochondrial dye JC-1 (our unpublished data). Brefeldin A (BFA) treatments were performed using 10 μg/ml brefeldin A according to Salazar *et al*. (2004a,b). Primary cultured mouse skin fibroblasts and immortalized *mocha* fibroblasts stably transfected with an empty retrovirus or a retrovirus carrying the AP-3 δ subunit (Peden *et al*., 2004) were grown in DMEM medium (Mediatech, Herndon, VA) (4.5 g/l glucose), supplemented with 10% fetal calf serum (Hyclone Laboratories, Logan, UT), 100 U/ml penicillin, and 100 μg/ml streptomycin (Mediatech), and hygromycin in cell carrying retroviruses (200 μg/ml).

Subcellular Fractionation and Vesicle Isolation

Supplemental Figure 1A depicts the purification strategy. Three independent preparations of vesicles were generated for mass spectrometry analysis. Cells were grown in 15-cm-diameter dishes (22 per experiment) to 80–90% confluence and treated overnight with 6 mM sodium butyrate before subcellular fractionation. Butyrate-containing media were removed, and cells were treated with methyl-β-cyclodextrin 10 mg/ml (7.6 mM) for 45 min at 37°C in serum-free DMEM media. After treatment cells were placed on ice, washed in cold phosphate-buffered saline, and harvested by sedimentation at 800 $\times$ *g* for 5 min at 4°C. Cell pellets were gently washed in intracellular buffer and homogenized with a 12-μm clearance cell cracker at 4°C in intracellular buffer (Clift-O'Grady *et al*., 1998) supplemented with Complete antiprotease mixture (Roche Diagnostics, Indianapolis, IN). Cell homogenates were sedimented at 1000 $\times$ *g* for 10 min to generate an S1 supernatant. S1 was spun at 25,000 $\times$ *g* for 45 min to generate a second supernatant S2. S2 fractions (2 mg/gradient) were further fractionated in a 5–25% glycerol gradient at 218,000 $\times$ *g* for 75 min in a SW55 rotor (Beckman Coulter, Fullerton, CA). Gradients were collected from the bottom in 17 fractions. Fractions were analyzed by immunoblot with synaptophysin, ZnT3, and tubulin antibodies. Peak fractions containing ZnT3 with a reduced content of synaptophysin and free of tubulin (8–11) were pooled and brought up to 45% sucrose plus Complete anti-protease mixture (3×). Then, 1.7 ml of this mixture containing ~20 μg of protein/gradient was laid in SW55 tubes and overlaid consecutively with 1.7 ml of 30 and 5% sucrose prepared in 20 mM MOPS-KOH, 0.5 mM $MgCl_2$, pH 7.2. Gradients were spun to equilibrium for 18 h at 180,000 $\times$ *g* in a SW55 rotor and collected from the top in 300-μl fractions. Fractions were analyzed by immunoblot to identify those with the highest ZnT3 content.

PC12 cell and brain fractionation in glycerol gradients was performed as described previously (Salazar *et al*., 2004b). S2 fractions were spun at 210,000 $\times$ *g* for 1 h in a Beckman TLA120.2 rotor to generate P3 membrane pellets. Immunomagnetic isolations were performed using methods detailed previously (Salazar *et al*., 2004a,b).

All gradient fractions were analyzed by immunoblot, and immunoreactivity was revealed by enhanced chemiluminescence. Immunoreactive bands were quantified using NIH Image 1.62 software as described previously (Salazar *et al*., 2004b).

Mass Spectrometry

For each vesicle preparation fraction 8 from ~12 equilibrium sucrose gradients was precipitated in ice with 10% trichloroacetic acid, and pellets were washed twice with ethanol/ether 1:1 (–20°C), dried, and resuspended in 0.1 N NaOH. Solubilized pellets were incubated in Laemmli sample buffer (Bio-Rad, Hercules, CA) at 70°C for 5 min, and proteins were resolved in a single lane of a 4–20% PAGE-SDS Criterion gel (Bio-Rad). Proteins were stained with colloidal Coomassie (Bio-Rad) to highlight the most abundant bands (usually 4–5) to guide the vertical slicing the entire gel lane. Subsequently, the lane was divided into 10 fractions. Each fraction was subjected to in-gel digestion with sequencing grade trypsin (Promega, Madison, WI) at 37°C overnight, and the peptides were extracted as described previously (Li *et al*., 1997).

For matrix-assisted laser desorption ionization (MALDI)/time of flight analysis, the tryptic peptides were desalted using a C18 ZipTip (Millipore, Billerica, MA) and analyzed by MALDI time-of-flight mass spectroscopy at the Emory Microchemical Core Facility using a Reflex III instrument (Bruker-Daltonics, Billerica, MA) as described by Hubalek *et al*. (2002). The observed ions were used to search the publicly available proteome for significant matches using the ProFound search engine (prowl.rockefeller.edu) specifying the Rodentia taxonomy. Further analysis was performed using postsource decay (Spengler, 1997). The resulting spectra were analyzed using the MASCOT search engine (www.matrixscience.com) and the National Center for Biotechnology Information nonredundant protein database search.

For nano-high-performance liquid chromatography (HPLC)-tandem mass spectrometry (MS/MS) analysis, a QSTAR XL (Applied Biosystems, Foster City, CA) hybrid quadrupole tandem mass spectrometer interfaced with an Ultimate nano-HPLC system (LC Packings, Sunnyvale, CA) was used. The mass spectrometer was operated in positive ion mode using information-dependent acquisition to acquire a single mass spectrometric (MS) scan (*m/z* 400-1900 scan range) followed by up to two MS/MS scans (*m/z* 50–1900 scan range). A rolling collision energy was used for the MS/MS scans. The data were analyzed using the ProID (Applied Biosystems) and MASCOT (www.matrixscience.com) search algorithms.

Due to the low yield of microvesicles, we defined the following criteria to consider a probable positive protein identification. Proteins were included for analysis 1) if represented by at least two peptides with a MASCOT score >45 or one peptide with a score >70 (defined from the antigen Thy1, entry 33; Supplemental Table 1, already known to be present in PC12 microvesicles; Jeng *et al*., 1998), and/or 2) if represented in two of the three spectrometry analyses. Peptides identified in a single MS run also were included if the corresponding proteins were part of a complex in which other subunits were identified in a distinct MS run (vacATPase, AP-3, synaptic vesicle proteins, and BLOCI). To test these inclusion criteria, we selected a group of proteins identified in a single MS analysis with low peptide counts (LAMP1, LAMP2, SV2, vimentin, RME8, KIAA1253, and TEM8), and we confirmed them as being present in AP-3-derived vesicles by either one of the following strategies: immunomagnetic isolation, defective targeting to microvesicles in *mocha* brain, or BFA-sensitive targeting to microvesicle fractions in PC12 cells (Supplemental Table 1; our unpublished data).

Microscopy

Immunofluorescence was performed as described previously (Salazar *et al*., 2004b). All cells were seeded on coverslips coated with Matrigel (BD Bio-

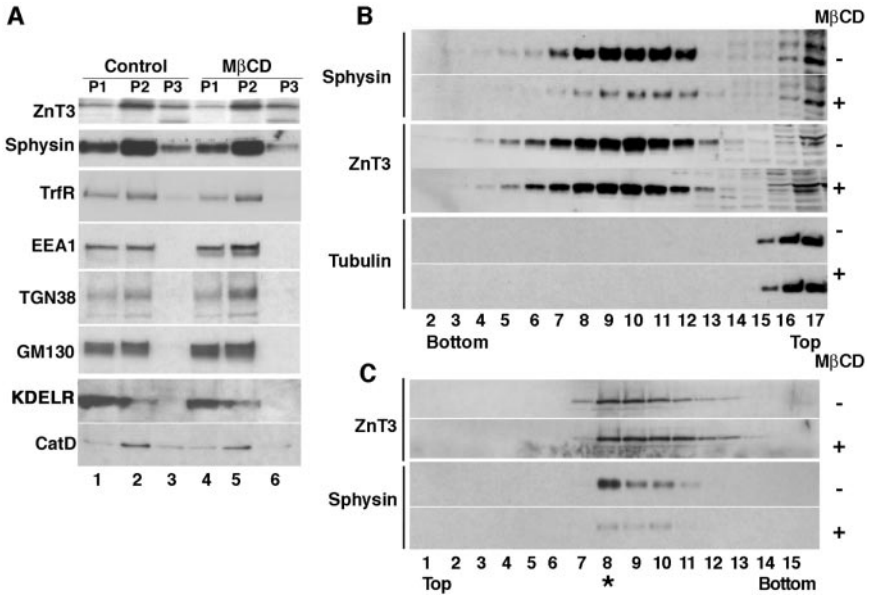

Figure 1. Isolation of a membrane fraction enriched in AP-3-derived vesicles. PC12 cells expressing ZnT3-HA were treated in the absence or presence of MβCD to interfere with SLMV biogenesis from plasma membrane. Plasma membrane-derived SLMV were monitored with synaptophysin and AP-3-derived vesicles with ZnT3. Cell homogenates were fractionated by differential centrifugation (A) to generate P1 (lanes 1 and 4), P2 (lanes 2 and 5), and P3 (lanes 3 and 6) membranes. P3 membranes contained the synaptic vesicle markers synaptophysin (Sphysin) and ZnT3, yet they were greatly depleted for other contaminating membranes. Cholesterol depletion did not affect the overall fractionation of Golgi, endosome, and lysosomes; however, it selectively decreased the synaptophysin content in P3 membranes (compare lanes 3 and 6). (B) Glycerol velocity gradient fractions probed with synaptophysin, ZnT3, and tubulin antibodies. The ZnT3-enriched peak is found in fractions 8–11, whereas the bulk of the cytosol, assessed with tubulin antibodies, remains in the top fractions (15–17). MβCD treatment decreases the synaptophysin content in SLMV fractions while sparing ZnT3. (C) Vesicles from glycerol fractions 8–11 were floated to equilibrium in sucrose gradients. ZnT3 and synaptophysin equilibrate at 26.4 $\pm$ 0.76% sucrose. MβCD treatment selectively decreases the synaptophysin content in SLMV without affecting ZnT3 (n = 3).

sciences). Images were acquired with a scientific-grade cooled charge-coupled device (Cool-Snap HQ with ORCA-ER chip) on a multiwavelength, widefield, three-dimensional microscopy system (Intelligent Imaging Innovations, Denver, CO), based on a 200M inverted microscope using a 63× numerical aperture 1.4 lens (Carl Zeiss, Thornwood, NY). Immunofluorescent samples were imaged at room temperature using a Sedat filter set (Chroma Technology, Rockingham, UT), in successive 0.25-μm focal planes. Out-of-focus light was removed with a constrained iterative deconvolution algorithm (Swedlow *et al*., 1997). MetaMorph quantification was performed as described previously (Salazar *et al*., 2004b).

Electron microscopy procedures are detailed in Salazar *et al*., 2004b. Immunoperoxidase staining on brain sections has been described in detail previously (Salazar *et al*., 2004a). All stainings were performed in duplicate in at least two independent experiments using two different monospecific affinity-purified phosphatidylinositol-4-kinase type IIα antibodies.

Cell Transfection and Flow Cytometry

PC12 cells were transfected with a PI4KIIα-pEGFP-N1 (a gift of Dr. T. Balla, Endocrinology and Reproduction Research Branch, National Institute of Child Health and Human Development, National Institutes of Health, Bethesda, MD) using Lipofectamine 2000 (Invitrogen, Carlsbad, CA). To generate PC12 expressing ZnT3 and PI4KIIα-green fluorescent protein (GFP), PC12 cells ZnT3 clone 4 (Salazar *et al*., 2004a) were transfected with pEGFP-PI4KIIα, and the pEF6/V5-His plasmid encoding the blasticidin-resistant gene (Invitrogen). Double transfectant clones were selected with 10 μg/ml blasticidin and 0.8 mg/ml G418.

Small Interference RNA (siRNA)

Cells were plated on coverslips and after 24 h, they were transfected in three consecutive days with 10 pmol (100 nM final concentration) of Dharmacon (Chicago, IL) SMARTPool siRNA (designed for accession NM_053735, containing an equimolar mix of the following oligos 5′GGUCAGAUCCUAAAUUUGA, 5′GAACCGACAGCUACUAUUG, 5′UAGUAUACCUGGCCAGUGA, and 5′CACCAAAGGUCGGGUCAUU), or Dharmacon siCONTROL nontargeting siRNA pool (containing an equimolar mix of the following oligos 5′AUGAACGUGAAUUGCUCAAUU, 5′UAAGGCUAUGAAGAGAUACUU, 5′AUGUAUUGGCCUGUAUUAGUU, 5′UAGCGACUAAACACAUCAAUU) using Lipofectamine 2000, following the manufacturer's (Invitrogen) protocol. Cells were fixed and processed for immunofluorescence 72 h after the initial transfection.

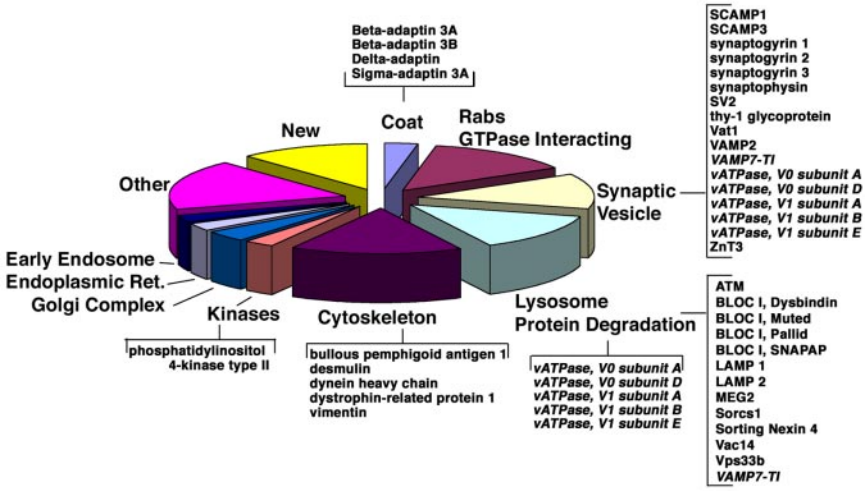

Figure 2. Classification of the ZnT3-enriched vesicle proteome. Relevant proteins for the categories described in Supplemental Table 1 are depicted in brackets. Entries in italics correspond to proteins described in both synaptic vesicles and lysosomes. For a complete list of all the proteins identified in the different categories refer to Supplemental Table 1.

RESULTS

Purification of AP-3-derived Vesicles

To further understand the cellular mechanisms converging upon and regulated by the adaptor complex AP-3, we sought to identify and isolate a subcellular fraction enriched in an AP-3-regulated membrane cargo, and therefore, most likely enriched in AP-3-derived vesicular carriers. We selected PC12 cells because, based on our previous studies, they offer unique advantages for this type of work. They possess well characterized and biochemically tractable AP-3- and AP-2-dependent vesicular traffic pathways. The latter generates synaptic-like microvesicles (SLMVs), organelles closely related to bona fide synaptic vesicles of neuronal synapses (Clift-O'Grady *et al*., 1990; Cameron *et al*., 1991). The former generates vesicles that share many similarities with SLMVs, but whose precise identity remains unclear. The AP-3 route can be examined by analyzing transfected ZnT3, an AP-3-interacting vesicle membrane protein (Salazar *et al*., 2004a,b). In contrast, the AP-2 pathway can be tracked by synaptophysin, a protein preferentially, yet not exclusively, targeted to SLMVs by AP-2-dependent mechanisms (Thiele *et al*., 2000; Salazar *et al*., 2004b). A central element to the isolation strategy presented here is the sensitivity of the AP-2 pathway to plasma membrane cholesterol depletion (Thiele *et al*., 2000; Salazar *et al*., 2004b). Pharmacological ablation of this pathway is detected as a pronounced and specific reduction of the synaptophysin levels in SLMVs without affecting the targeting of ZnT3 to a microvesicle population (Salazar *et al*., 2004a,b).

We used PC12 cells expressing a C-terminal HA tagged version of ZnT3 (Salazar *et al*., 2004a,b). Furthermore, MβCD was used to deplete cholesterol and therefore to disrupt the biogenesis of SLMVs, whose sedimentation characteristics overlap with that of AP-3-derived vesicles. Cells were incubated in either the absence or presence of MβCD and were gently homogenized and fractionated by differential centrifugation to obtain a 25,000 $\times$ *g* S2 supernatant (Supplemental Figure 1A) and a total membrane pellet derived from the S2 fraction (P3) (Figure 1A, P3, lane 3). Cholesterol depletion did not affect the overall subcellular distribution of organelle markers in these primary subfractions such as the endosomal markers transferrin receptor and EEA1, the Golgi markers TGN38 and GM130, the endoplasmic reticulum protein KDEL receptor, and the lysosomal marker cathepsin D (Figure 1A, compare lanes 1–2 and 4–5). It also did not affect the distribution of ZnT3. However, MβCD treatment selectively decreased the synaptophysin content in the P3 fraction, which is enriched in small vesicles, consistent with the reported effect of this compound on SLMV biogenesis (Thiele *et al*., 2000; Salazar *et al*., 2004b) (Figure 1A, compare lanes 3 and 6). S2, rather than P3 was chosen for further fractionation due to the difficulty of achieving an efficient resuspension of the dense P3 pellet. Most of the S2 fraction is represented by cytosolic proteins, but these are efficiently separated from membranes in velocity and density gradients.

Glycerol velocity gradients discriminate vesicles by size and resolve ZnT3-enriched vesicles from several other major contaminants (Figure 1B). In these gradients, most cytosolic proteins, for example tubulin, stayed at the top of the gradient (Figure 1B and Supplemental Figure 1B, fractions 14–17). The bulk of synaptophysin (primarily SLMVs) and ZnT3 (i.e., an AP-3-derived cargo) migrated to the middle of glycerol gradients where ~0.3% of the homogenate protein was recovered (Supplemental Figure 1B, inset, fractions 8–11). Importantly, the content of synaptophysin in the ZnT3-containing fractions was substantially reduced after MβCD treatment (Figure 1B) without affecting ZnT3 content (Figure 1B). As shown previously (Thiele *et al*., 2000; Salazar *et al*., 2004b), the MβCD effects were not restricted to synaptophysin among SLMV proteins, suggesting that recovery of AP-2-generated SLMVs in this fraction is disrupted by plasma membrane cholesterol extraction.

We further purified a ZnT3-enriched microvesicle fraction from the ZnT3-enriched peak of the glycerol gradient using isopycnic sedimentation. Fractions 8–11 of the glycerol gradient were pooled and fractionated by equilibrium flotation in sucrose gradients (Supplemental Figure 1). Most of the protein remained at the bottom of the gradient (Supplemental Figure 1C, fractions 12–16), possibly reflecting either protein aggregates comigrating with size-isolated microvesicles in the glycerol gradient or proteins loosely attached to these membranes. A small percentage (0.5%) of the protein floated to a portion of the gradient (Supplemental Figure 1C, 26.4 $\pm$ 0.76% sucrose, asterisk) enriched in ZnT3

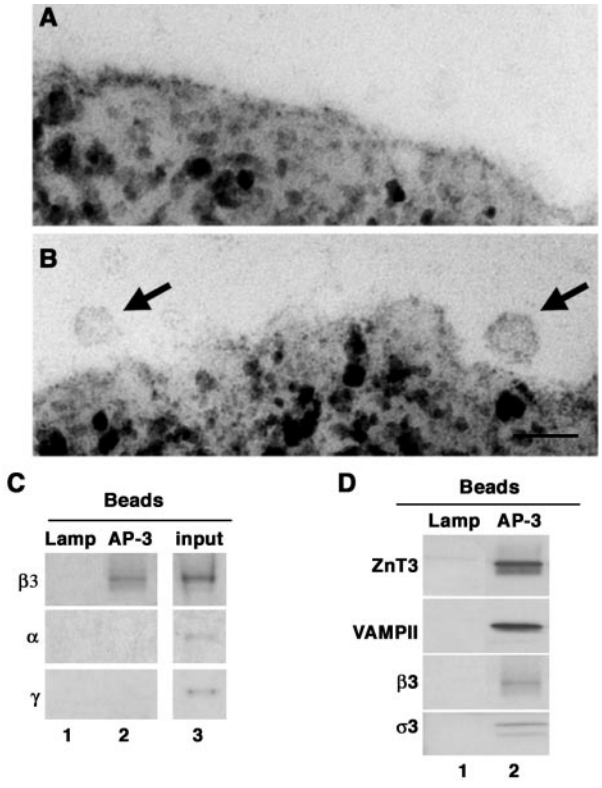

Figure 3. Identification of AP-3-derived vesicles. Vesicle fractions isolated by sequential glycerol and sucrose sedimentation were immunomagnetically isolated with beads coated with either a luminal human-specific Lamp1 antibody or AP-1 γ as controls, or coated with antibodies against AP-3 δ adaptin. Beads were analyzed by transmission electron microscopy (A and B) or immunoblot (C and D). AP-1 γ beads did not bind membranes (A). AP-3 δ beads bind 40-nm vesicles (see arrows) (B). Bar, 55 nm. (C) AP-3 vesicles are free of AP-1 or AP-2 adaptins. β3 Adaptin blots were exposed for 3 min. α and γ Adaptin blots were exposed overnight. (D) AP-3-coated vesicles contain synaptic vesicle markers. Membranes bound to beads coated with antibodies against the indicated antigens were resolved in SDS-PAGE and analyzed by immunoblot with antibodies against synaptic vesicle proteins (ZnT3 and VAMP II) and the AP-3 subunits β3 and σ3. Control immunoisolations in C and D, lane 1, were performed with LAMP antibodies. Input corresponds to 10%.

and synaptophysin (Figure 1C, asterisk). Importantly, most of the synaptophysin equilibrating at 26.4% sucrose was sensitive to cholesterol depletion, yet the ZnT3 content of this fraction remained unaffected (Figure 1C). As predicted, silver staining of this ZnT3-positive peak sucrose fraction revealed a significant reduction of the protein content in material from MβCD-treated cells (Supplemental Figure 1D, asterisk, and E, compare left and right lanes), providing further evidence that MβCD treatment not only affected synaptophysin sorting but also, more generally, the generation of vesicles comigrating with AP-3.

In summary, we have prepared a vesicle fraction of homogenous small size (glycerol velocity gradient) and density (sucrose gradient), which is enriched in ZnT3, an AP-3-interacting vesicle protein and a known cargo of AP-3-derived vesicles. When obtained from cells treated with MβCD, this fraction is deenriched in SLMVs, which have similar sedimentation properties. Although this fraction is still expected to be heterogeneous, it can function as a useful starting point to search for new proteins sorted by AP-3. We carried out its proteomic analysis to validate the enrichment of AP-3-sorted cargo and to identify new potential components of such vesicles.

Proteomic Analysis of the Fraction Enriched in AP-3-derived Vesicles

The protein composition of the ZnT3-enriched vesicle fraction obtained from cholesterol-depleted cells was examined by tandem mass spectrometry. Analysis of three independent vesicle preparations (Supplemental Figure 1) identified 137 proteins (Figure 2 and Supplemental Table 1). Notably, among these proteins were four subunits of the AP-3 complex (entries 1–4). These included the neuronal and ubiquitous AP-3 β3 isoforms. The former is implicated in the biogenesis of a subset of synaptic vesicles (Faundez *et al*., 1998; Nakatsu *et al*., 2004; Salazar *et al*., 2004b; Seong *et al*., 2005), the latter is involved in the biogenesis of lysosome and lysosome-related organelles (Dell'Angelica, 2004). Importantly, no subunits of AP-1 and AP-2 adaptors were detected, either by mass spectrometry or immunoblot analysis (Supplemental Figure 2A; see below). We determined that AP-3 was concentrated 16.5 times in ZnT3 fractions compared with crude P1 membranes (Supplemental Figure 2, B and C), suggesting the presence of at least partial AP-3 coats. Based on their flotation properties (migration at 27% sucrose), however, these vesicles are not expected to be fully coated AP-3 vesicles, because such vesicles migrate at 39.7 $\pm$ 1.3% sucrose (Faundez *et al*., 1998). The AP-3-containing small vesicle fraction also could be identified in untransfected PC12 cells (our unpublished data) and rat brain (Supplemental Figure 3). Velocity and equilibrium density sedimentation of rat brain small membrane fractions (Supplemental Figure 1A) revealed a population of ZnT3/VAMPII-containing vesicles that cosedimented with the AP-3 σ3 subunit and was devoid of AP-1 positive membranes (Supplemental Figure 3). These results validate our vesicle purification scheme and provide evidence for the enrichment of AP-3-derived vesicles in the fraction.

Several classes of proteins were identified in the fraction, predictably many proteins implicated in vesicular transport. Many of them were synaptic vesicle membrane proteins (Figure 2 and Supplemental Table 1, entries 26–41) and molecules involved in the biogenesis/regulation of synaptic vesicles (Figure 2 and Table 1; for examples, see entries 5, 6, 105, and 107). Consistent with the presence of ubiquitous AP-3 complexes containing the β3A subunit, ~17% of the proteins identified could be assigned to the category of lysosomes/lysosome-related organelles, which included AP-3 cargoes (LAMP1 and LAMP2) and BLOC-I complex subunits (Figure 2 and Supplemental Table 1). Some proteins, such as vacuolar proton pump subunits and vesicle-associated membrane protein (VAMP)7/TI-VAMP are

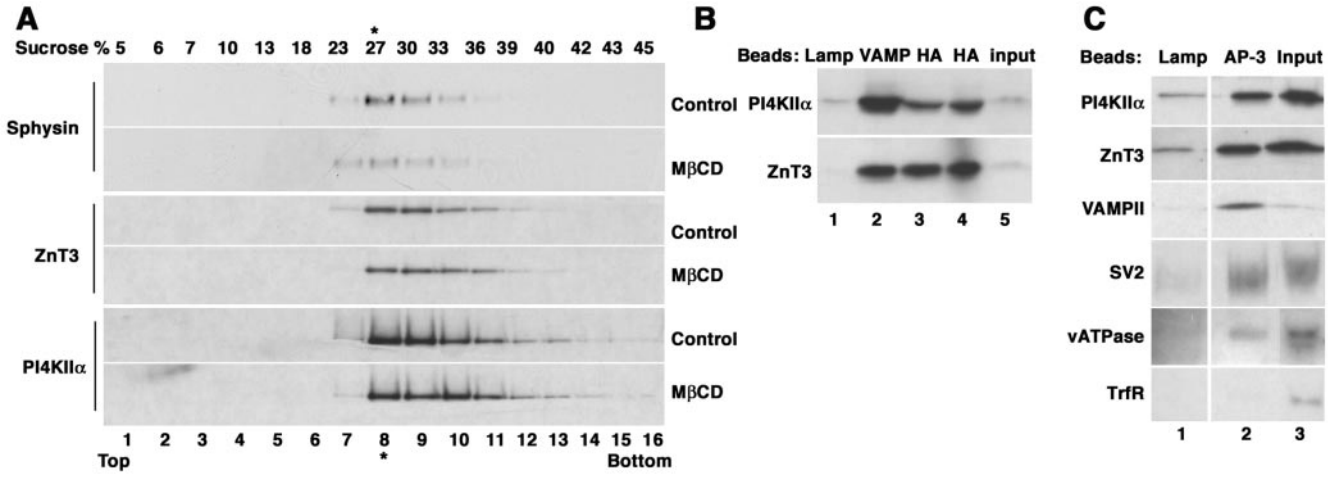

Figure 4. PI4KIIα is present in AP-3-derived vesicles. (A) PC12 cells expressing ZnT3-HA were treated in the absence or presence of MβCD, and ZnT3-enriched fractions were isolated by sequential velocity and isopycnic sedimentation. Fractions were analyzed by immunoblot with antibodies against synaptophysin, ZnT3, and PI4KIIα. The kinase comigrated with ZnT3. The abundance of this kinase was not affected by MβCD treatment. (B) PI4KIIα is present in vesicles containing synaptic vesicle markers. Vesicles were isolated with magnetic beads decorated with control (luminal domain of LAMP, lane 1), VAMP II (lane 2), or HA (lanes 3 and 4) antibodies to recognize the tag in ZnT3. Bound vesicle content was analyzed by immunoblot with kinase and ZnT3 antibodies. (C) PI4KIIα is present in AP-3-coated vesicles. Vesicles were bound to beads coated with either a luminal human-specific Lamp I antibody as negative control, or coated with antibodies against AP-3 δ adaptin. PI4KIIα is present in AP-3-coated vesicles together with synaptic vesicle markers (ZnT3, VAMPII, SV2, and vacuolar ATPase). No contamination with transferrin receptor was detected in the AP-3-coated vesicles. Transferrin receptor blot was exposed 20 times longer that the other blots. Vesicles used in B and C were isolated by velocity sedimentation from untreated cells. Inputs represent 10%.

present both in synaptic vesicles (synaptic vesicle subpopulations in the case of VAMP7/TI-VAMP) and lysosomes (Advani *et al*., 1999; Martinez-Arca *et al*., 2003; Muzerelle *et al*., 2003). Interestingly, VAMP7-TI-VAMP was shown to be sorted by AP-3-dependent mechanisms (Martinez-Arca *et al*., 2003). An abundant protein previously implicated in Golgi (Wang *et al*., 2003), endosome (Balla *et al*., 2002), and synaptic vesicle traffic (Guo *et al*., 2003) was PI4KIIα (GI16758554; Figure 2 and Supplemental Table 1, entry 82). This enzyme was represented by a cumulative count of 38 peptides. In agreement with the AP-3-intermediate filament interaction recently described by one of our laboratories (Styers *et al*., 2004), several proteins identified were functionally linked to intermediate filament cytoskeleton assembly and dynamics. However, abundant cytoskeletal proteins such as tubulin and actin were not detected in this fraction (Figure 1 and Supplemental Table 1; data not shown). Peptides representing Rab GTPases were particularly numerous in this fraction, and the peptide representation of Rab1 suggested the presence of vesicles involved in endoplasmic reticulum-to-Golgi transport. Resident proteins of the endoplasmic reticulum and the Golgi complex collectively represented 6.5% of all the proteins identified. However, we failed to detect by immunoblot the KDEL receptor as well as GM130 or TGN38 (our unpublished data).

The AP-3 subunits identified by MS/MS were physically associated with the vesicles as revealed by immunomagnetic isolation of microvesicles from the ZnT3-enriched fraction with beads decorated with anti-AP-3 δ subunit antibodies. Electron microscopy analysis detected the presence of homogeneously sized vesicles (~40 nm) bound to these beads but not to controls beads decorated by anti-AP-1 γ subunit antibodies (Figure 3 compare A and B). Immunoblot analysis of the membranes bound to the beads coated with AP-3 δ subunit antibodies revealed presence not only of β3 (Figure 3, C and D, lane 2) but also σ3 adaptins (Figure 3D, lane 2). Vesicles containing AP-3 were free of α and γ adaptins, indicating that the AP-3 complex was selectively bound to these membranes. In addition, partially coated AP-3 vesicles also contained vesicle proteins such as ZnT3 and synaptobrevin/VAMPII. These proteins were not retrieved by beads coated with control antibodies (antibodies directed against a luminal LAMP epitope; Figure 3, C and D, LAMP, lane 1).

PI4KIIα Is Present in AP-3-derived Vesicles

Our goal was to use the proteomic analysis of a ZnT3-enriched membrane fraction to identify potential new components of AP-3-derived vesicles. The abundance of PI4KIIα in the fraction (Table 1, entry 82) and its critical importance in a metabolic pathway strongly linked to vesicle biogenesis/function (Wang *et al*., 2003) prompted us to focus on this protein in this first study. This kinase is not an intrinsic membrane protein, but it is tightly bound to membranes, at least partially via a lipid anchor (Barylko *et al*., 2001). It has

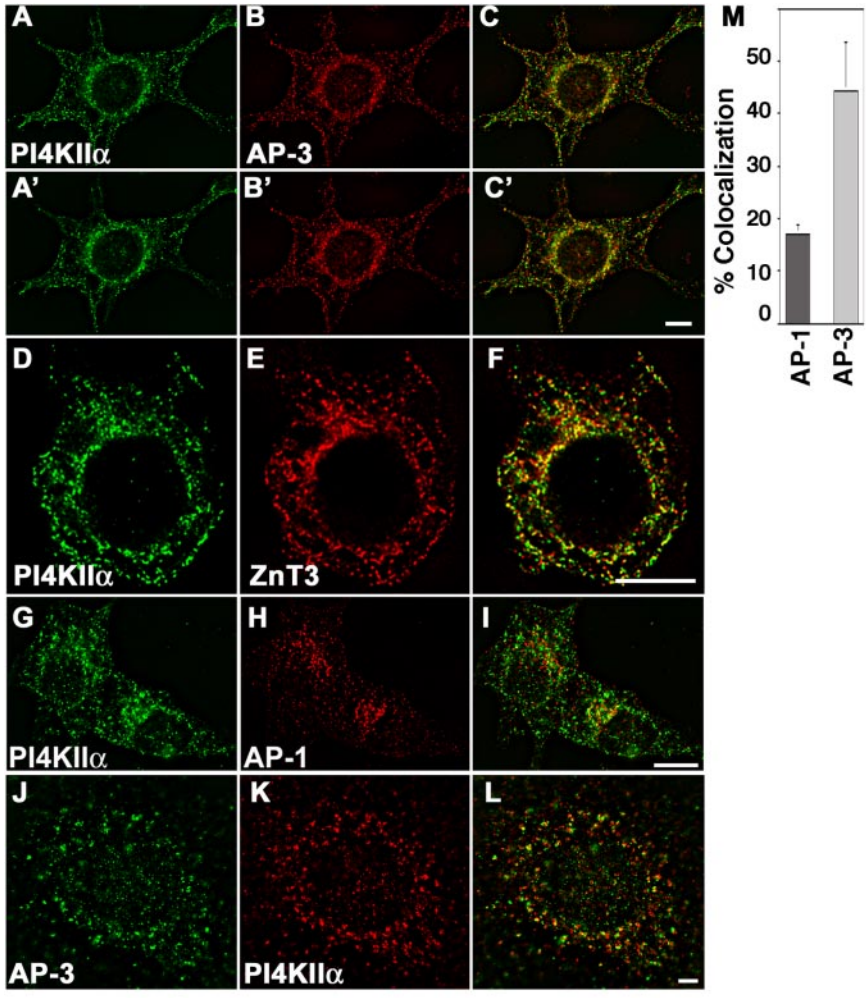

Figure 5. PI4KIIα colocalizes predominantly with AP-3 and its cargo ZnT3. PC12 cells expressing HA-tagged ZnT3 were costained with antibodies against PI4KIIα (A and A′, D, and G) and either AP-3 δ adaptin (B and B′), HA antibodies to detect ZnT3 (E), or AP-1 γ adaptin (H). Similarly, primary mouse skin fibroblasts were stained with AP-3 δ and PI4KIIα antibodies (J–L). Cells were imaged by wide field deconvolution microscopy. (M) Colocalization of PI4KIIα and the adaptor complexes was determined by MetaMorph. The kinase extensively colocalizes with AP-3 and ZnT3 and to a lower extent with AP-1. A–C to A′–C′ series represent two optical planes taken every 0.75 μm. Bar, 6 μm.

been described in the Golgi complex (Wang *et al*., 2003), synaptic vesicles (Guo *et al*., 2003), and endosomes (Balla *et al*., 2002), an organelle that in PC12 cell gives raise to microvesicles by AP-3-dependent mechanisms (Faundez *et al*., 1997; Shi *et al*., 1998; Blagoveshchenskaya *et al*., 1999; Salazar *et al*., 2004a,b). As a first step to determine the potential localization of PI4KIIα to AP-3-derived vesicles, fractions from PC12 cell glycerol velocity gradients and isopycnic sucrose gradients leading to the ZnT3-enriched vesicle preparation (Figure 1C) were probed with antibodies directed against PI4KIIα. In both gradients (Figures 4A and 6A, respectively, control strips) PI4KIIα comigrated with ZnT3 and, in contrast with synaptophysin, such migration was resistant to plasma membrane cholesterol depletion (Figure 4A). The kinase was physically associated with ZnT3 vesicles as determined by organelle immunoisolation experiments. Beads coated with antibodies directed against the cytosolic tail of VAMPII (Figure 4B, lane 2) or against the HA epitope of transfected ZnT3 (Figure 4B, lanes 3 and 4) as well as beads coated with control antibodies (anti-lumenal domain of Lamp) were incubated with ZnT3-enriched glycerol gradient fractions. PI4KIIα was recovered both in ZnT3 and in VAMPII immunoabsorbed material but was virtually undetectable in control immunoisolations (Figure 4B, compare lanes 1 with 2–4). Furthermore, PI4KIIα was present in AP-3-positive vesicles because this protein was recovered bound to beads decorated with AP-3 δ antibodies together with ZnT3, VAMPII, SV2, and the p116 subunit of the vacuolar ATPase (Figure 4C, compare lanes 1 and 2). Similar results were obtained with microvesicles isolated from untransfected P12 cells (our unpublished data). Moreover, the PI4KIIα-positive vesicles were free of the early endosome marker transferrin receptor (Figure 4C), a membrane protein known to be excluded from SLMV fractions containing AP-2-derived vesicles (Clift-O'Grady *et al*., 1990; Lichtenstein *et al*., 1998) and from AP-3-derived vesicles (Dell'Angelica *et al*., 1999; Peden *et al*., 2004; Salazar *et al*., 2004b). The presence of PI4KIIα in AP-3-positive organelles was supported by wide-field deconvolution immunofluorescence microscopy of wild-type PC12 cells (Figure 5, A–C and G–I) or cells transfected with HA-tagged ZnT3 (Figure 5, D–F). Endogenous PI4KIIα immunoreactivity had a punctate pattern that partially overlapped with AP-3 (Figure 5, A–C′) and ZnT3 immunoreactivity (Figure 5, D–F). PI4KIIα has been reported to colocalize with AP-1 (Wang *et al*., 2003); therefore, we analyzed the extent of kinase colocalization with AP-1 (Figure 5, G–I) and AP-3 adaptors in PC12 cells. Seventeen percent of the PI4KIIα colocalized with AP-1-positive compartments. In contrast, PI4KIIα colocalization with AP-3 was 2.6 times more prominent (Figure 5M). We also examined the colocalization of PI4KIIα with AP-3 in primary cultured mouse skin fibroblasts. Similarly, to PC12 cells, the kinase extensively colocalized with AP-3 (Figure 5, J–L) in wild-type fibroblasts and in mocha fibroblasts rescued by reexpresion of the delta adaptin AP-3 subunit (Figure 8). In summary, our results support the hypothesis that PI4KIIα preponderantly resides in organelles that contain AP-3 and

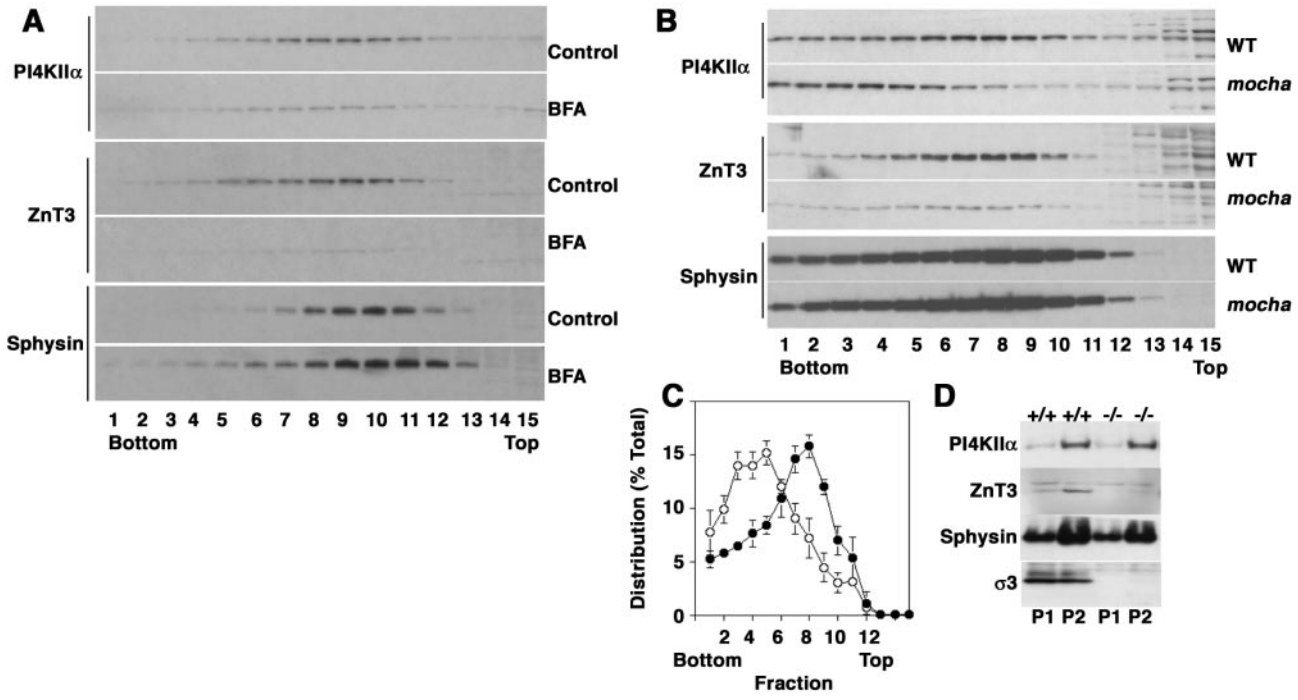

Figure 6. PI4KIIα is targeted by AP-3-dependent mechanisms. (A) PC12 cells were treated either in the absence or presence of brefeldin A to deplete AP-3-generated vesicles and were subsequently fractionated in glycerol velocity gradients. Synaptophysin levels were not affected by brefeldin A; in contrast, ZnT3 and PI4KIIα levels were dramatically reduced (n = 2). (B) High-speed supernatants (S2) from wild-type and *mocha* brain homogenates were fractionated in glycerol gradients to resolve synaptic vesicles and AP-3 vesicles. Synaptic vesicle antigen levels across gradients were determined by immunoblot using antibodies against PI4KIIα, ZnT3, and synaptophysin (Sphysin). PI4KIIα and ZnT3 sedimentation pattern and the antigen content in membranes were specifically altered in *mocha* brain vesicles. (C) Depicts the normalized content distribution of PI4KIIα (n = 4). Closed circles represent wild-type membranes, and open circles correspond to *mocha* vesicles. (D) Distribution of synaptic vesicle antigens in P1 and P2 membranes from wild-type (+/+) and *mocha* brain (−/−).

AP-3 cargoes both in neuronal and nonneuronal cells, thus validating the results of the proteomic analysis.

AP-3-dependent Targeting of PI4KIIa

To further elucidate the relation between AP-3 and PI4KIIα, we investigated whether the subcellular distribution of the kinase was sensitive to pharmacological and genetic manipulations that affect AP-3 function. We first analyzed the effects of BFA on PI4KIIα targeting in PC12 cells. This drug blocks AP-1 (Robinson and Kreis, 1992) and AP-3 recruitment to membranes and robustly inhibits the formation of vesicles generated by AP-3-dependent mechanisms (Faundez *et al*., 1997; Shi *et al*., 1998; Blagoveshchenskaya *et al*., 1999; Salazar *et al*., 2004a,b). In contrast, it does not affect formation of AP-2-derived SLMVs (Faundez *et al*., 1997; Shi *et al*., 1998; Blagoveshchenskaya *et al*., 1999; Salazar *et al*., 2004a,b). As expected, the ZnT3 containing peak in glycerol velocity gradients almost disappeared after BFA treatment. In addition, it produced a similar effect on PI4KIIα, whereas synaptophysin remained unaffected by the drug treatment (Figure 6A).

To further explore a role of AP-3 in PI4KIIα targeting to vesicles, we examined whether such targeting is perturbed in the AP-3-null *mocha* mouse (Kantheti *et al*., 1998). AP-3-derived synaptic vesicles and bona fide synaptic vesicles fractions sediment as a symmetric peak in glycerol velocity gradients from extracts of wild-type mouse brain. PI4KIIα, ZnT3, and synaptophysin comigrate with this peak (Figure 6B). Notably, in AP-3-deficient *mocha* brain, PI4KIIα was redistributed to a faster migrating membrane fraction (Figure 6, B and C; n = 4). We determined that in the absence of AP-3 at least half of the kinase (47.4 ± 8%; n = 4) was shifted from the fractions most enriched in ZnT3 (fractions 7–9) to faster migrating fractions. Importantly, the effects of the *mocha* allele upon PI4KIIα synaptic vesicle targeting were specific because synaptophysin content and distribution were not affected by the absence of functional AP-3 (Figure 6B). This decrease was due to a redistribution of the kinase rather than global changes in brain kinase expression, because kinase content was not detectably modified in P1-P2 brain fractions (Figure 6D).

The effects of the *mocha* mutation on the subcellular distribution of PI4KIIα are similar to those reported for ZnT3 and for another synaptic vesicle protein whose traffic is regulated by AP-3: chloride channel 3 (ClC3) (Salazar *et al*., 2004a). ZnT3 and ClC3 targeting defects also are manifested as a decreased content of these proteins in a subset of nerve terminals in situ (Salazar *et al*., 2004a), such as in nerve terminals of the hippocampus (Salazar *et al*., 2004a; Seong *et al*., 2005). Therefore, we explored whether the PI4KIIα content in mouse brain nerve terminals was similarly affected by the *mocha* mutation. Immunostaining of wild-type and *mocha* brain hippocampal sections revealed a reduction in PI4KIIα immunoreactivity in the mossy fiber nerve terminals of the hilus (Figure 7, A–D) and CA3 region (Figure 7, E–H). These nerve terminals were previously shown to be enriched in ZnT3 (Palmiter *et al*., 1996) and ClC-3 (Stobrawa *et al*., 2001) in wild-type, but not in *mocha* mice (Salazar *et al*., 2004a). The decreased kinase immunostaining in mossy nerve terminals was not due to a "global" change in nerve terminal number or structure because VAMPII distribution and abundance were not affected by the *mocha* mutation (Figure 7, I and J).

The disrupting effects of the *mocha* mutation on the subcellular distribution of PI4KIIα also were observed in fibroblasts derived from *mocha* mice. For these experiments, the localization of PI4KIIα and its relation to other organelle markers was analyzed by deconvolution immunofluorescence and quantified by MetaMorph software (Figure 8). Wild-type (Figure 5) and *mocha* cells rescued by retroviral expression of the AP-3 subunit delta adaptin were used as controls. Whereas in cells rescued by reexpression of delta adaptin PI4KIIα partially colocalized with AP-3 and the

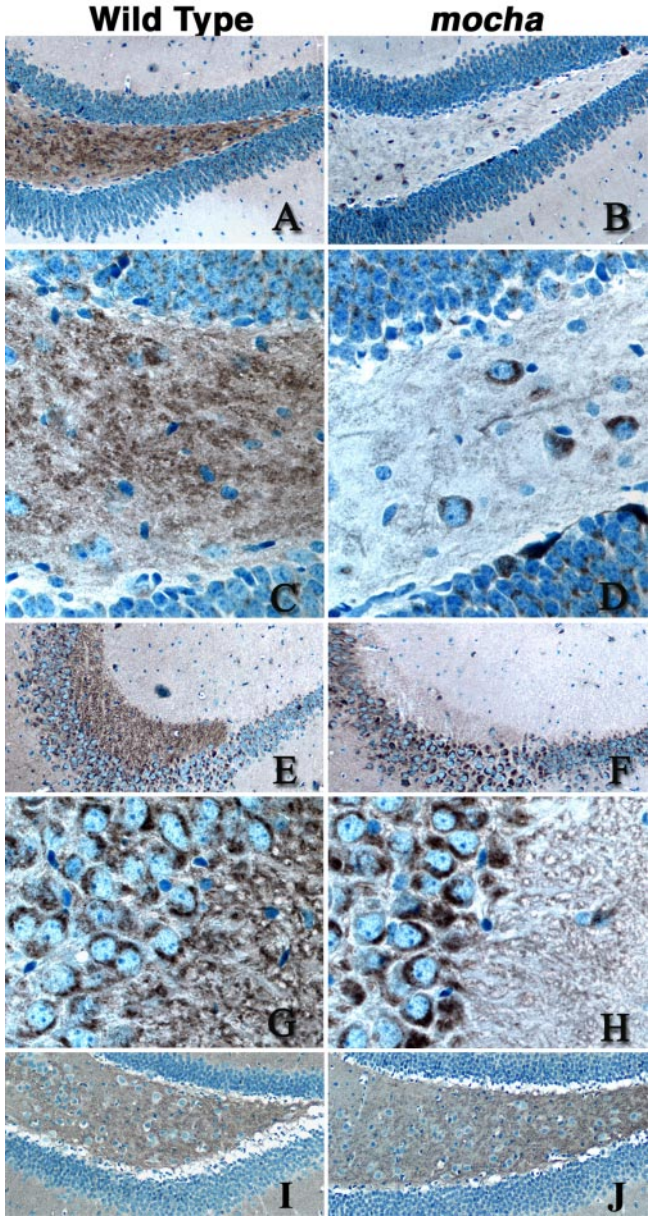

Figure 7. PI4KIIα content decreases in *mocha* hippocampal mossy fiber nerve terminals. Wild-type (A, C, E, G, and I) and *mocha* (B, D, F, H, and J) hippocampal brains sections were stained with antibodies against PI4KIIα (A–H), and VAMP II (I–J). Immunocomplexes were detected with the ABC peroxidase reagent and DAB deposition. (A–D) Representative images of the dentate gyrus and hilus at low (A and B, 20×) and high magnification (C and D, 63×), whereas E–H correspond to the CA3 region of the hippocampus acquired at low (E–F) or high power (G–H). Note the reduction of PI4KIIα immunoreactivity in the hilus mossy fibers and CA3 mossy fiber synaptic terminals. Images are representative of sections obtained from four wild-type and *mocha* brains simultaneously stained in three independent experiments using either of two PI4KIIα antibodies.

AP-3 cargo LAMP1 (35.9 ± 4.5%; n = 10), this colocalization was reduced in the absence of AP-3 (Figure 8, A and C), and the bulk of PI4KIIα was redistributed to the perinuclear region in *mocha* cells. Concomitantly with this, the colocalization between PI4KIIα and AP-1 increased 3.4-fold in *mocha* cells (Figure 8B). These results indicate that PI4KIIα subcellular distribution is regulated in part by AP-3 complexes both in neuronal and nonneuronal cells.

AP-3 Function Is Regulated by PI4KIIa

Phosphatidylinositol kinases regulate vesicle formation both in the exocytic and endocytic pathways (De Matteis and Godi, 2004; Wenk and De Camilli, 2004). Thus, a reciprocal functional relationship between PI4KIIα and AP-3 is plausible, with the enzymatic activity of PI4KIIα modulating AP-3–dependent vesicle formation. For example, PI(4)P generated by PI4KIIα may regulate AP-3 recruitment to membranes (De Matteis and Godi, 2004; Wenk and De Camilli, 2004). We tested this hypothesis by analyzing whether decreased levels of PI4KIIα affected the distribution of AP-3

PC12 cell PI4KIIα expression was down-regulated by oligonucleotide-mediated siRNA using rat PI4KIIα specific sequences (Figure 9). Controls were performed using transfection reagent alone or unrelated oligonucleotide sequences. PI4KIIα was down-regulated to 50% of the endogenous levels compared with control oligonucleotide-transfected cells analyzed by Western blotting (Figure 9, A and B; n = 8). However, upon immunofluorescence analysis, the knockdown of PI4KIIα seemed to be heterogeneous, suggesting that in a subpopulation of cells the down-regulation of the kinase was much >50%. These effects were selective because the levels of β-actin and transferrin receptor remained unchanged (Figure 9B). The characteristic perinuclear localization of AP-3 observed in control siRNA-treated PC12 cells (Figure 9, C and D) was lost in cells with reduced levels of PI4KIIα and much of the cytoplasmic vesicular staining was diminished (Figure 9D, asterisk). This phenotype, designated "disperse," was observed in two-thirds of the PI4KIIα-knocked down cells (Figure 9C), but in very few of the control oligonucleotide-transfected cells (9%), thus arguing against nonspecific oligonucleotide effects (our unpublished data).

To analyze the role of PI4KIIα in the biogenesis of AP-3-derived vesicles, we generated stable PC12 cell clones differing in PI4KIIα-GFP expression yet possessing identical levels of ZnT3 (Figure 10A). We performed subcellular frac-

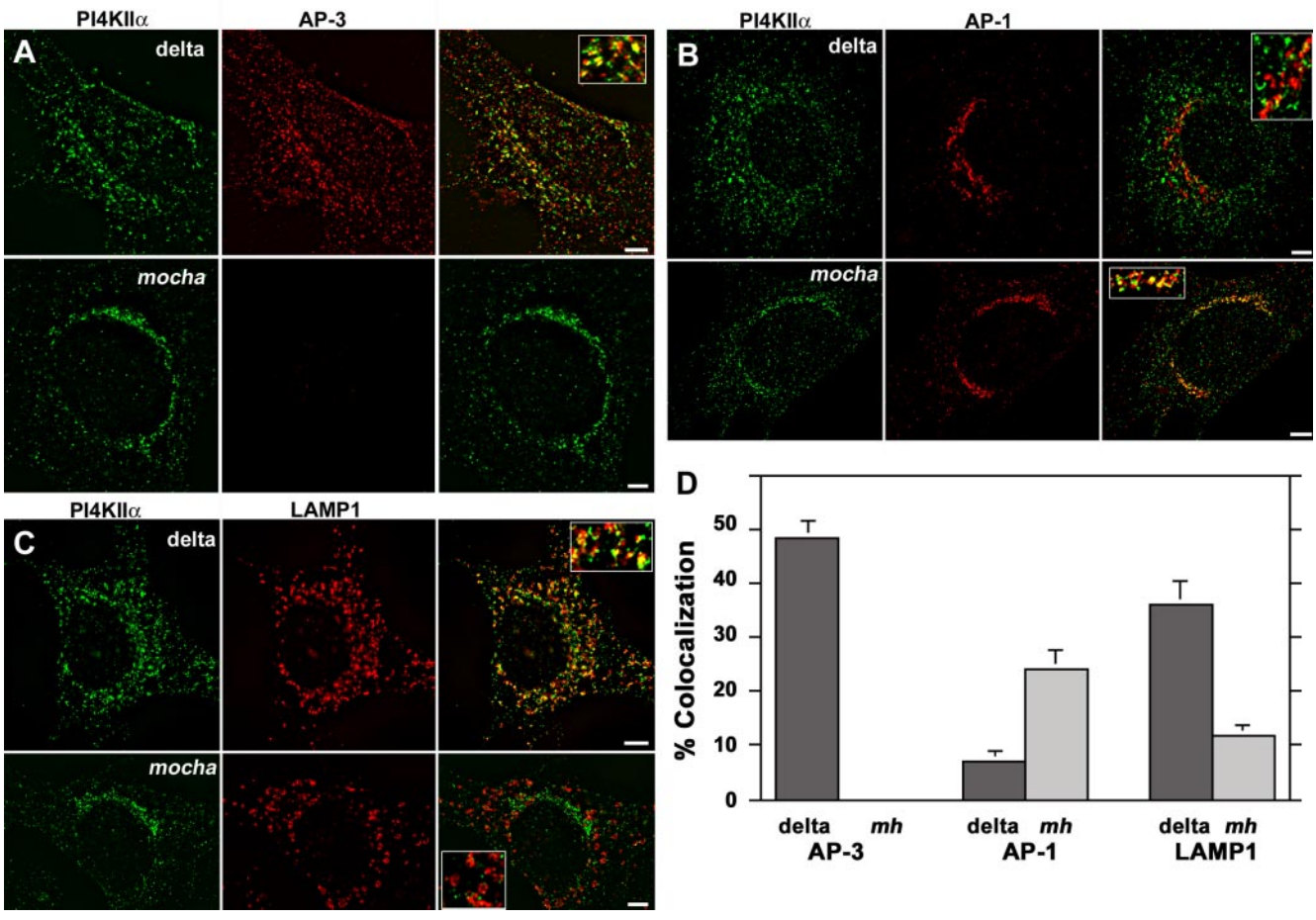

Figure 8. PI4KIIα redistributes to perinuclear compartments in the absence of AP-3. *Mocha* mouse fibroblasts transduced with retroviruses carrying the δ subunit (delta) or without insert (*mocha*, *mh*) were double labeled with antibodies against PI4KIIα (A–D) and one of the following antigens: AP-3 δ adaptin (A), AP-1 γ adaptin (B), and the AP-3 cargo LAMP1 (C). Cells were imaged by wide field deconvolution microscopy, and the extent of colocalization was determined in at least 10 randomly selected cells collected from two independent experiments for each condition (D). In the absence of AP-3 (*mocha*, *mh*), PI4KIIα redistributes to perinuclear compartments increasing it colocalization with AP-1 and decreasing its localization with the AP-3 cargo LAMP-1. Bars, 5 μm.

tionation to determine whether increased kinase expression induced a redistribution of ZnT3 (Figure 10B, P3). Indeed, PI4KIIα overexpression increased the content of ZnT3 (and VAMP2) in P3 fractions (Figure 10B, compare lanes 3 and 6). Importantly, an increase in AP-3 in these fractions also was observed. Transferrin receptor remained unaffected, suggesting that the observed effects were not a result of nonselective vesiculation of organelles. These results were corroborated by the analysis of P3 membranes on glycerol velocity gradients. In PI4KIIα-GFP-expressing cells, the recovery of endogenous PI4KIIα (asterisk), AP-3, and ZnT3 was increased in this fraction (Figure 10C). Similar results were obtained in two clonal cell lines (our unpublished data) and in PC12 cells transiently transfected with PI4KIIα-GFP (our unpublished data). These results are consistent with the hypothesis that PI4KIIα regulates membrane recruitment and sorting function of AP-3 complexes.

DISCUSSION

In the present study, we have used a proteomic approach to identify new components of AP-3-derived vesicles. We have identified PI4KIIα as one of such components, and we show that PI4KIIα and AP-3 control in a reciprocal manner their subcellular localization.

We have used a homogeneous cell system (PC12 cells) engineered to express ZnT3, a well established cargo of these vesicles (Salazar *et al*., 2004a,b; Seong *et al*., 2005). A combination of velocity and isopycnic centrifugation from cells depleted of cholesterol to disrupt biogenesis of AP-2-derived vesicles resulted in the generation of a microvesicle fraction highly enriched in ZnT3. This fraction, although composed of microvesicles homogenous in size and density, is still expected to be biochemically heterogeneous. In fact, its proteomic analysis revealed the presence of markers for a variety of vesicular carriers implicated in different transport reactions. However, its enrichment in AP-3-derived vesicles was confirmed by the presence of predicted components of such vesicles.

The lysosomal proteins detected in our vesicle preparation did not include soluble hydrolases but comprised a variety of membrane proteins previously shown to interact with AP-3 either biochemically or genetically. This finding is consistent with an involvement of AP-3 in the targeting of membrane proteins to lysosomes. We detected the AP-3 cargo proteins LAMP 1, 2, and TI-VAMP/VAMP7 (Bonifacino and Traub, 2003; Martinez-Arca *et al*., 2003), an AP-3–interacting protein that regulates lysosome content (ATM) (Lim *et al*., 1998; Barlow *et al*., 2000), proteins related to pigment dilution genes (vps33b) (Stepp *et al*., 1997), and gene products affected in pigment dilution/Hermansky–Pudlak syndrome (BLOC I subunits pallid, muted, SNAPAP, and dysbindin/sandy) (Dell'Angelica, 2004). The presence of BLOC1 in AP-3-derived vesicles provides a mechanistic explanation to the overlapping phenotypes observed in mice and humans harboring mutations in either AP-3 or BLOC I subunits (Dell'Angelica, 2004).

The presence of a set of synaptic vesicle proteins in the ZnT3-enriched fraction may reflect comigration of PC12 synaptic vesicles (SLMVs) not disrupted by the cholesterol depletion but also the bona fide presence of these proteins in AP-3-derived vesicles (Figures 3 and 4). Whereas AP-3 is clearly not required for the generation of the bulk of synaptic vesicles either in PC12 cells (Salazar *et al*., 2004b) or in neurons (Kantheti *et al*., 1998; Salazar *et al*., 2004b), its role in the biogenesis of a subpopulation of synaptic vesicles is supported by studies of mice deficient in neuron-specific AP-3 subunits (Nakatsu *et al*., 2004; Seong *et al*., 2005). In these mice, synaptic vesicle-associated proteins such as ZnT3, ClC-3, and the vesicular GABA-transporter are either present at reduced levels or mislocalized (Nakatsu *et al*., 2004; Seong *et al*., 2005). Synaptic vesicles are enriched in nerve terminals, where they are continuously regenerated by membrane recycling, whereas lysosomes are selectively

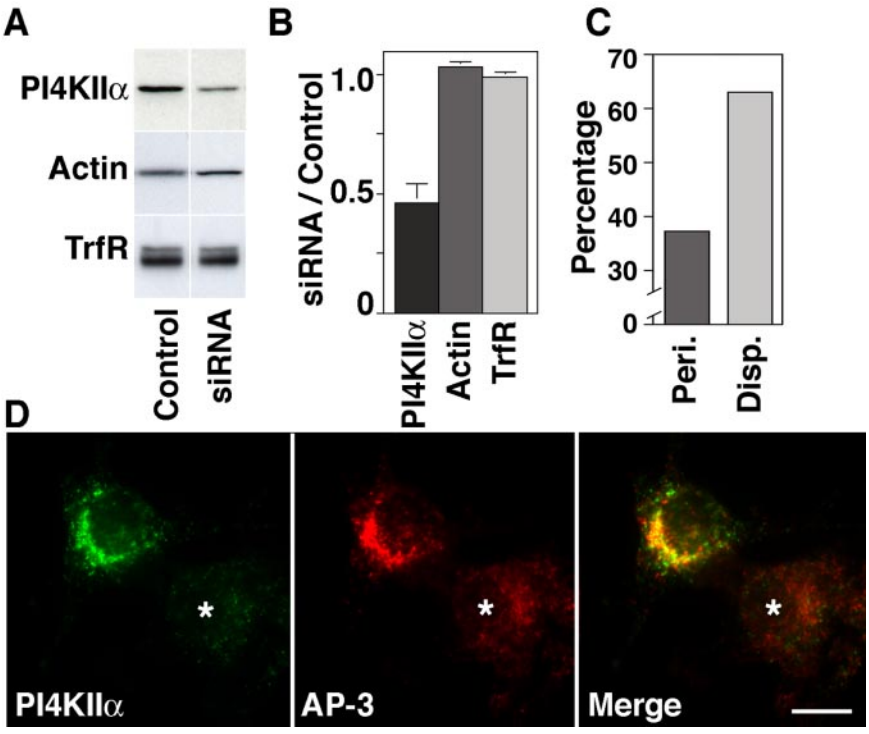

Figure 9. PI4KIIα siRNA alters the subcellular distribution of AP-3 complexes. (A) Rat-specific PI4KIIα siRNA and control oligonucleotide-transfected PC12 cells were analyzed by immunoblot with antibodies against PI4KIIα, actin, and transferrin receptor (TrfR). (B) PI4KIIα siRNA selectively reduced kinase content by 50% of control values (n = 8). (C and D) Rat-specific PI4KIIα siRNA-treated PC12 cells were stained with antibodies against PI4KIIα and AP-3 delta subunit and examined by immunomicroscopy. Kinase down-regulation was observed only in PI4KIIα siRNA-transfected cells (asterisk). Reduction of the cell PI4KIIα levels resulted in disappearance of AP-3 from perinuclear (peri.) membranous compartments adopting a disperse appearance (disp.). (C) Phenotypes were scored in 113 cells collected in three independent experiments. Bar, 5 μm.

localized in cell bodies and dendrites and are excluded from axons and axon terminals. However, it has been shown that neuron-specific AP-3 subunits are present in axons (Seong *et al*., 2005) and that some membrane proteins such as TI-VAMP/VAMP7, the vacuolar proton pump, ClC3, Cln3, and the Niemann–Pick type C1 protein are present both on lysosomes and on subpopulations of axonal vesicles (Luiro *et al*., 2001; Stobrawa *et al*., 2001; Li *et al*., 2002; Karten *et al*., 2003; Muzerelle *et al*., 2003; Kyttala *et al*., 2004a,b). Interestingly, TI-VAMP/VAMP7 and Cln3 have been reported to be trafficked by AP-3-dependent mechanisms (Martinez-Arca *et al*., 2003; Kyttala *et al*., 2004b). Thus, a key question is how neuronal and ubiquitous AP-3 complexes may be involved in the biogenesis of lysosomes, synaptic vesicles, and the traffic of a subset of lysosomal proteins to axonal organelles.

The goal of this study was to identify new important components of AP-3-derived vesicles. We found PI4KIIα to be enriched in the ZnT3-enriched fraction from cholesterol-depleted PC12 cells. We provide evidence for a functional association between the kinase and AP-3 analyzing whether the kinase is targeted by AP-3-dependent mechanisms and whether the kinase expression levels control the subcellular distribution of AP-3 and its vesicle formation function. PI4KIIα lacks transmembrane regions, but it is tightly associated with membranes via covalently conjugated fatty acids (Barylko *et al*., 2001). In agreement with the presence of PI4KIIα on AP-3-derived vesicles, we observed partial colocalization of AP-3 and the kinase. In addition, the kinase sedimentation pattern in subcellular fractionation from PC12 cells was not affected by cholesterol depletion, a manipulation that affects AP-2-dependent sorting (Thiele *et al*., 2000; Salazar *et al*., 2004b), but it was instead affected by brefeldin A. PI4KIIα was previously implicated in AP-1-dependent sorting as well (Wang *et al*., 2003), and it is therefore of interest that AP-1 recruitment also is affected by brefeldin A (Robinson and Kreis, 1992).

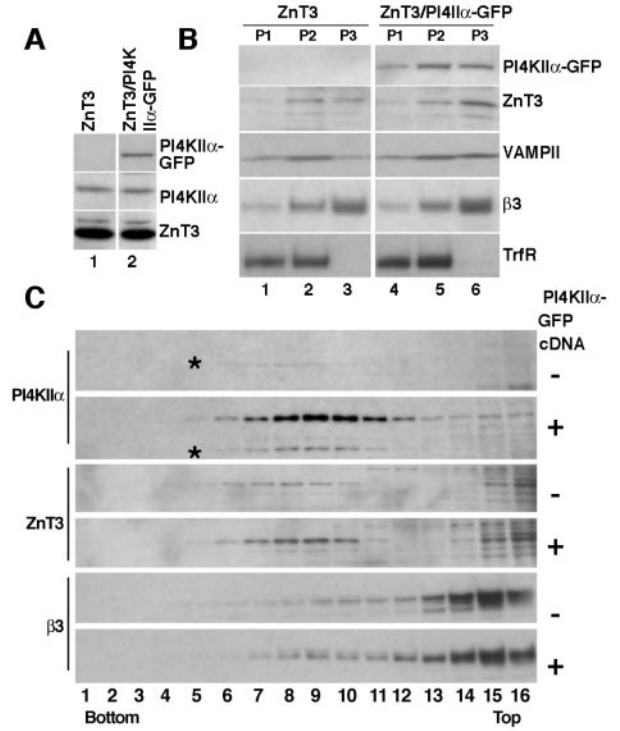

Figure 10. Overexpression of PI4KIIα increases the recovery of AP-3-derived vesicles. PC12 clone 4 cells expressing ZnT3 were transfected with GFP-tagged PI4KIIα. (A) Double transfected clonal cells expressing PI4KIIα-GFP and similar amounts of ZnT3 and endogenous PI4KIIα were selected and further analyzed by subcellular fractionation. (B) Cells were fractionated by differential sedimentation to obtain a P3 fraction. Expression of PI4KIIα shifts ZnT3, VAMPII, and β3 adaptin from endosome-containing P2 fractions to P3 membranes, which are enriched in small vesicles, without obvious changes in the sedimentation pattern of the transferrin receptor (TrfR). (C) P3 membranes contained in S2 fractions were fractionated by glycerol velocity sedimentation. Fractions were probed with antibodies against PI4KIIα, ZnT3, and AP-3 β3 adaptin. Kinase expression increases the content of synaptic vesicle markers and AP-3 in microvesicle fractions (n = 3). All gradients were probed with antibodies against tubulin to confirm equal loading.

The subcellular fractionation and localization of PI4KIIα were abnormal in skin fibroblasts and brain tissue of *mocha* mice. Although the total level of PI4KIIα was not decreased in these mice compared with control, its concentration in nerve terminals of hippocampus mossy fibers was strikingly decreased. Interestingly, these nerve terminals are those where the most severe changes in AP-3 cargoes, such as ZnT3 and ClC3, were previously observed in *mocha* mice (Salazar *et al*., 2004a,b; Seong *et al*., 2005). Changes in subcellular distribution of PI4KIIα were observed in *mocha* fibroblasts, where the punctate PI4KIIα immunoreactivity present throughout the cells, but not the perinuclear immunoreactivity, was lost. These results suggest that a significant pool of PI4KIIα is controlled by the function of the adaptor complex AP-3. We note that PI4KIIα was reported to interact with CD63 (Berditchevski *et al*., 1997; Yauch and Hemler, 2000), a membrane protein of lysosomes proposed to be sorted by AP-3-dependent mechanisms (Rous *et al*., 2002). Thus, it is possible that a direct or indirect interaction with CD63 may account, at least in part, for the localization of PI4KIIα in AP-3-derived vesicles.

PI4KIIα has been described in a subpopulation of endosomes (Balla *et al*., 2002), synaptic vesicles (Guo *et al*., 2003), and in the Golgi complex (Guo *et al*., 2003; Wang *et al*., 2003). In the Golgi complex, PI4KIIα was shown to control the generation of a pool of phosphatidylinositol-4-phosphate [PI(4)P] that participates in the recruitment of the clathrin adaptor AP-1 (Guo *et al*., 2003; Wang *et al*., 2003). Our findings in *mocha* mice clearly exclude the possibility that the kinases' presence in ZnT3-enriched vesicle fractions is simply the result of contamination by AP-1-derived Golgi complex vesicles. We have confirmed that PI4KIIα colocalizes with AP-1 in PC12 cells and skin fibroblasts. Interestingly, in the absence of AP-3 complexes (*mocha*), the kinase redistributes to the Golgi area, increasing its colocalization with AP-1 by ~350%. These results suggest that the steady-state localization of PI4KIIα reflects an equilibrium between Golgi and endosomal compartments. This model provides a potential explanation for discrepancies in the reported subcellular localization of PI4KIIα (Balla *et al*., 2002; Wang *et al*., 2003).

Our results also provide evidence that PI4KIIα regulates the subcellular distribution and function of AP-3 adaptors, possibly reflecting a role of PI(4)P [or PI(4)P metabolites] analogous to the role of PI(4)P in AP-1 recruitment (Wang *et al*., 2003). The AP-3 complex bound to intracellular compartments diminishes concomitantly with the reduction on the PI4KIIα levels by siRNA. Furthermore, increasing kinase expression in PC12 cells increases the recovery of AP-3, ZnT3, and the endogenous kinase present in ZnT3-enriched microvesicles. Interestingly, in PC12 cells overexpressing PI4KIIα, the increased recovery of ZnT3 in the putative AP-3-derived fraction was paralleled by an increased recovery of synaptic vesicle proteins that was not sensitive to

cholesterol depletion (Salazar and Faundez, unpublished data). Collectively, our results strongly support a functional link between PI4KIIα and the AP-3 complex. PI4KIIα, via its enzymatic activity, may directly enhance AP-3 binding to membranes, or may act indirectly, by recruiting other proteins that promote AP-3 recruitment and function. Based on the function of PI4KIIα and PI(4)P in AP-1 recruitment (Wang *et al*., 2003) and of PI(4)P-5-kinases and phosphatidylinositol 4,5-bisphosphate in AP-2 binding to membranes (Krauss *et al*., 2003; Wenk and De Camilli, 2004), we favor a mechanism in which PI(4)P or one of its metabolites regulate directly AP-3 binding to membranes.

ACKNOWLEDGMENTS

We are indebted to the Faundez laboratory members and Drs. A. H. Kowalczyk, S. W. L'Hernault, and E.M.A. Werner for comments. This work was supported by National Institutes of Health Grants NS42599, and NS36251 (to V. F. and P.D.C., respectively) and by a grant from the Emory Center for Research on Complementary Medicine in Neurodegenerative Diseases (to V. F.).

REFERENCES

Advani, R. J., Yang, B., Prekeris, R., Lee, K. C., Klumperman, J., and Scheller, R. H. (1999). VAMP-7 mediates vesicular transport from endosomes to lysosomes. J. Cell Biol. *146*, 765–776.

Balla, A., Tuymetova, G., Barshishat, M., Geiszt, M., and Balla, T. (2002). Characterization of type II phosphatidylinositol 4-kinase isoforms reveals association of the enzymes with endosomal vesicular compartments. J. Biol. Chem. *277*, 20041–20050.

Barlow, C., *et al*. (2000). ATM is a cytoplasmic protein in mouse brain required to prevent lysosomal accumulation. Proc. Natl. Acad. Sci. USA *97*, 871–876.

Barylko, B., Gerber, S. H., Binns, D. D., Grichine, N., Khvotchev, M., Sudhof, T. C., and Albanesi, J. P. (2001). A novel family of phosphatidylinositol 4-kinases conserved from yeast to humans. J. Biol. Chem. *276*, 7705–7708.

Benson, K. F., *et al*. (2003). Mutations associated with neutropenia in dogs and humans disrupt intracellular transport of neutrophil elastase. Nat. Genet. *35*, 90–96.

Berditchevski, F., Tolias, K. F., Wong, K., Carpenter, C. L., and Hemler, M. E. (1997). A novel link between integrins, transmembrane-4 superfamily proteins (CD63 and CD81), and phosphatidylinositol 4-kinase. J. Biol. Chem. *272*, 2595–2598.

Blagoveshchenskaya, A. D., Hewitt, E. W., and Cutler, D. F. (1999). Di-leucine signals mediate targeting of tyrosinase and synaptotagmin to synaptic-like microvesicles within PC12 cells. Mol. Biol. Cell *10*, 3979–3990.

Blondeau, F., *et al*. (2004). Tandem MS analysis of brain clathrin-coated vesicles reveals their critical involvement in synaptic vesicle recycling. Proc. Natl. Acad. Sci. USA *101*, 3833–3838.

Bonifacino, J. S., and Glick, B. S. (2004). The mechanisms of vesicle budding and fusion. Cell *116*, 153–166.

Bonifacino, J. S., and Traub, L. M. (2003). Signals for sorting of transmembrane proteins to endosomes and lysosomes. Annu. Rev. Biochem. *72*, 395–447.

Cameron, P. L., Sudhof, T. C., Jahn, R., and De Camilli, P. (1991). Colocalization of synaptophysin with transferrin receptors: implications for synaptic vesicle biogenesis. J. Cell Biol. *115*, 151–164.

Clark, R. H., Stinchcombe, J. C., Day, A., Blott, E., Booth, S., Bossi, G., Hamblin, T., Davies, E. G., and Griffiths, G. M. (2003). Adaptor protein 3-dependent microtubule-mediated movement of lytic granules to the immunological synapse. Nat. Immunol. *4*, 1111–1120.

Clift-O'Grady, L., Desnos, C., Lichtenstein, Y., Faundez, V., Horng, J. T., and Kelly, R. B. (1998). Reconstitution of synaptic vesicle biogenesis from PC12 cell membranes. Methods *16*, 150–159.

Clift-O'Grady, L., Linstedt, A. D., Lowe, A. W., Grote, E., and Kelly, R. B. (1990). Biogenesis of synaptic vesicle-like structures in a pheochromocytoma cell line PC-12. J. Cell Biol. *110*, 1693–1703.

De Matteis, M. A., and Godi, A. (2004). PI-loting membrane traffic. Nat. Cell Biol. *6*, 487–492.

Dell'Angelica, E. C. (2004). The building BLOC(k)s of lysosomes and related organelles. Curr. Opin. Cell Biol. *16*, 458–464.

Dell'Angelica, E. C., Mullins, C., Caplan, S., and Bonifacino, J. S. (2000). Lysosome-related organelles. FASEB J. *14*, 1265–1278.

Dell'Angelica, E. C., Shotelersuk, V., Aguilar, R. C., Gahl, W. A., and Bonifacino, J. S. (1999). Altered trafficking of lysosomal proteins in Hermansky-Pudlak syndrome due to mutations in the beta 3A subunit of the AP-3 adaptor. Mol. Cell *3*, 11–21.

Faundez, V., Horng, J. T., and Kelly, R. B. (1997). ADP ribosylation factor 1 is required for synaptic vesicle budding in PC12 cells. J. Cell Biol. *138*, 505–515.

Faundez, V., Horng, J. T., and Kelly, R. B. (1998). A function for the AP3 coat complex in synaptic vesicle formation from endosomes. Cell *93*, 423–432.

Faundez, V., and Kelly, R. B. (2000). The AP-3 complex required for endosomal synaptic vesicle biogenesis is associated with a casein kinase Iα-like isoform. Mol. Biol. Cell *11*, 2591–2604.

Feng, L., *et al*. (1999). The beta3A subunit gene (Ap3b1) of the AP-3 adaptor complex is altered in the mouse hypopigmentation mutant pearl, a model for Hermansky-Pudlak syndrome and night blindness. Hum. Mol. Genet. *8*, 323–330.

Guo, J., Wenk, M. R., Pellegrini, L., Onofri, F., Benfenati, F., and De Camilli, P. (2003). Phosphatidylinositol 4-kinase type IIα is responsible for the phosphatidylinositol 4-kinase activity associated with synaptic vesicles. Proc. Natl. Acad. Sci. USA *100*, 3995–4000.

Hubalek, F., Edmondson, D. E., and Pohl, J. (2002). Synthesis and characterization of a collagen model δ-*O*-phosphohydroxylysine-containing peptide. Anal. Biochem. *306*, 124–134.

Jeng, C. J., McCarroll, S. A., Martin, T. F., Floor, E., Adams, J., Krantz, D., Butz, S., Edwards, R., and Schweitzer, E. S. (1998). Thy-1 is a component common to multiple populations of synaptic vesicles. J. Cell Biol. *140*, 685–698.

Kanaseki, T., and Kadota, K. (1969). The "vesicle in a basket". A morphological study of the coated vesicle isolated from the nerve endings of the guinea pig brain, with special reference to the mechanism of membrane movements. J. Cell Biol. *42*, 202–220.

Kantheti, P., Diaz, M. E., Peden, A. E., Seong, E. E., Dolan, D. F., Robinson, M. S., Noebels, J. L., and Burmeister, M. L. (2003). Genetic and phenotypic analysis of the mouse mutant mh(2J), an Ap3d allele caused by IAP element insertion. Mamm. Genome *14*, 157–167.

Kantheti, P., *et al*. (1998). Mutation in AP-3 delta in the mocha mouse links endosomal transport to storage deficiency in platelets, melanosomes, and synaptic vesicles. Neuron *21*, 111–122.

Karten, B., Vance, D. E., Campenot, R. B., and Vance, J. E. (2003). Trafficking of cholesterol from cell bodies to distal axons in Niemann Pick C1-deficient neurons. J. Biol. Chem. *278*, 4168–4175.

Krauss, M., Kinuta, M., Wenk, M. R., De Camilli, P., Takei, K., and Haucke, V. (2003). ARF6 stimulates clathrin/AP-2 recruitment to synaptic membranes by activating phosphatidylinositol phosphate kinase type Iγ. J. Cell Biol. *162*, 113–124.

Kyttala, A., Ihrke, G., Vesa, J., Schell, M. J., and Luzio, J. P. (2004a). Two motifs target Batten disease protein CLN3 to lysosomes in transfected nonneuronal and neuronal cells. Mol. Biol. Cell *15*, 1313–1323.

Kyttala, A., Yliannala, K., Schu, P., Jalanko, A., and Luzio, J. P. (2004b). AP-1 and AP-3 facilitate lysosomal targeting of batten disease protein CLN3 via its dileucine motif. J. Biol. Chem. *280*, 10277–10283.

Li, G., Waltham, M., Anderson, N. L., Unsworth, E., Treston, A., and Weinstein, J. N. (1997). Rapid mass spectrometric identification of proteins from two-dimensional polyacrylamide gels after in gel proteolytic digestion. Electrophoresis *18*, 391–402.

Li, X., Wang, T., Zhao, Z., and Weinman, S. A. (2002). The ClC-3 chloride channel promotes acidification of lysosomes in chinese hamster ovary-K1 and Huh-7 cells. Am. J. Physiol. *282*, C1483–C1491.

Lichtenstein, Y., Desnos, C., Faundez, V., Kelly, R. B., and Clift-O'Grady, L. (1998). Vesiculation and sorting from PC12-derived endosomes in vitro. Proc. Natl. Acad. Sci. USA *95*, 11223–11228.

Lim, D. S., Kirsch, D. G., Canman, C. E., Ahn, J. H., Ziv, Y., Newman, L. S., Darnell, R. B., Shiloh, Y., and Kastan, M. B. (1998). ATM binds to beta-adaptin in cytoplasmic vesicles. Proc. Natl. Acad. Sci. USA *95*, 10146–10151.

Luiro, K., Kopra, O., Lehtovirta, M., and Jalanko, A. (2001). CLN3 protein is targeted to neuronal synapses but excluded from synaptic vesicles: new clues to Batten disease. Hum. Mol. Genet. *10*, 2123–2131.

Martinez-Arca, S., *et al*. (2003). A dual mechanism controlling the localization and function of exocytic v-SNAREs. Proc. Natl. Acad. Sci. USA *100*, 9011–9016.

Maycox, P. R., Link, E., Reetz, A., Morris, S. A., and Jahn, R. (1992). Clathrin-coated vesicles in nervous tissue are involved primarily in synaptic vesicle recycling. J. Cell Biol. *118*, 1379–1388.

Muzerelle, A., Alberts, P., Martinez-Arca, S., Jeannequin, O., Lafaye, P., Mazie, J. C., Galli, T., and Gaspar, P. (2003). Tetanus neurotoxin-insensitive vesicle-associated membrane protein localizes to a presynaptic membrane compartment in selected terminal subsets of the rat brain. Neuroscience *122*, 59–75.

Nakatsu, F., *et al*. (2004). Defective function of GABA-containing synaptic vesicles in mice lacking the AP-3B clathrin adaptor. J. Cell Biol. *167*, 293–302.

Palmiter, R. D., Cole, T. B., Quaife, C. J., and Findley, S. D. (1996). ZnT-3, a putative transporter of zinc into synaptic vesicles. Proc. Natl. Acad. Sci. USA *93*, 14934–14939.

Pearse, B. M. (1975). Coated vesicles from pig brain: purification and biochemical characterization. J. Mol. Biol. *97*, 93–98.

Pearse, B. M., and Crowther, R. A. (1987). Structure and assembly of coated vesicles. Annu. Rev. Biophys. Biophys. Chem. *16*, 49–68.

Peden, A. A., Oorschot, V., Hesser, B. A., Austin, C. D., Scheller, R. H., and Klumperman, J. (2004). Localization of the AP-3 adaptor complex defines a novel endosomal exit site for lysosomal membrane proteins. J. Cell Biol. *164*, 1065–1076.

Pfeffer, S. R., and Kelly, R. B. (1981). Identification of minor components of coated vesicles by use of permeation chromatography. J. Cell Biol. *91*, 385–391.

Pfeffer, S. R., and Kelly, R. B. (1985). The subpopulation of brain coated vesicles that carries synaptic vesicle proteins contains two unique polypeptides. Cell *40*, 949–957.

Ritter, B., Blondeau, F., Denisov, A. Y., Gehring, K., and McPherson, P. S. (2004). Molecular mechanisms in clathrin-mediated membrane budding revealed through subcellular proteomics. Biochem. Soc. Trans. *32*, 769–773.

Robinson, M. S. (2004). Adaptable adaptors for coated vesicles. Trends Cell Biol. *14*, 167–174.

Robinson, M. S., and Kreis, T. E. (1992). Recruitment of coat proteins onto Golgi membranes in intact and permeabilized cells: effects of brefeldin A and G protein activators. Cell *69*, 129–138.

Rous, B. A., Reaves, B. J., Ihrke, G., Briggs, J. A., Gray, S. R., Stephens, D. J., Banting, G., and Luzio, J. P. (2002). Role of adaptor complex AP-3 in targeting wild-type and mutated CD63 to lysosomes. Mol. Biol. Cell *13*, 1071–1082.

Salazar, G., Love, R., Styers, M. L., Werner, E., Peden, A., Rodriguez, S., Gearing, M., Wainer, B. H., and Faundez, V. (2004a). AP-3-dependent mechanisms control the targeting of a chloride channel (ClC-3) in neuronal and non-neuronal cells. J. Biol. Chem. *279*, 25430–25439.

Salazar, G., Love, R., Werner, E., Doucette, M. M., Cheng, S., Levey, A., and Faundez, V. (2004b). The zinc transporter ZnT3 interacts with AP-3 and it is targeted to a distinct synaptic vesicle subpopulation. Mol. Biol. Cell *15*, 575–587.

Salem, N., Faundez, V., Horng, J. T., and Kelly, R. B. (1998). A v-SNARE participates in synaptic vesicle formation mediated by the AP3 adaptor complex. Nat. Neurosci. *1*, 551–556.

Seong, E., Wainer, B. H., Hughes, E. D., Saunders, T. L., Burmeister, M., and Faundez, V. (2005). Genetic analysis of the neuronal and ubiquitous AP-3 adaptor complexes reveals divergent functions in brain. Mol. Biol. Cell *16*, 128–140.

Shi, G., Faundez, V., Roos, J., Dell'Angelica, E. C., and Kelly, R. B. (1998). Neuroendocrine synaptic vesicles are formed in vitro by both clathrin-dependent and clathrin-independent pathways. J. Cell Biol. *143*, 947–955.

Spengler, B. (1997). Post-source decay analysis in matrix-assisted laser desorption/ionization mass spectrometry of biomolecules. J. Mass Spectrom. *32*, 1019–1036.

Stepp, J. D., Huang, K., and Lemmon, S. K. (1997). The yeast adaptor protein complex, AP-3, is essential for the efficient delivery of alkaline phosphatase by the alternate pathway to the vacuole. J. Cell Biol. *139*, 1761–1774.

Stobrawa, S. M., *et al*. (2001). Disruption of ClC-3, a chloride channel expressed on synaptic vesicles, leads to a loss of the hippocampus. Neuron *29*, 185–196.

Styers, M. L., Salazar, G., Love, R., Peden, A. A., Kowalczyk, A. P., and Faundez, V. (2004). The endo-lysosomal sorting machinery interacts with the intermediate filament cytoskeleton. Mol. Biol. Cell *15*, 5369–5382.

Swedlow, J. R., Sedat, J. W., and Agard, D. A. (1997). Deconvolution in optical microscopy. In: Deconvolution of Images and Spectra, ed. P. A. Jansson, San Diego: Academic Press, 284–307.

Taylor, S. W., Fahy, E., and Ghosh, S. S. (2003). Global organellar proteomics. Trends Biotechnol. *21*, 82–88.

Thiele, C., Hannah, M. J., Fahrenholz, F., and Huttner, W. B. (2000). Cholesterol binds to synaptophysin and is required for biogenesis of synaptic vesicles. Nat. Cell Biol. *2*, 42–49.

Wang, Y. J., Wang, J., Sun, H. Q., Martinez, M., Sun, Y. X., Macia, E., Kirchhausen, T., Albanesi, J. P., Roth, M. G., and Yin, H. L. (2003). Phosphatidylinositol 4 phosphate regulates targeting of clathrin adaptor AP-1 complexes to the Golgi. Cell *114*, 299–310.

Wenk, M. R., and De Camilli, P. (2004). Protein-lipid interactions and phosphoinositide metabolism in membrane traffic: insights from vesicle recycling in nerve terminals. Proc. Natl. Acad. Sci. USA *101*, 8262–8269.

Yauch, R. L., and Hemler, M. E. (2000). Specific interactions among transmembrane 4 superfamily (TM4SF) proteins and phosphoinositide 4-kinase. Biochem. J. *351*, 629–637.